



Semiclassical fifth virial coefficients for improved *ab initio* helium-4 standards

Katherine R. S. Shaul^a, Andrew J. Schultz^a, David A. Kofke^{a,*}, Michael R. Moldover^b

^a Department of Chemical and Biological Engineering, University at Buffalo, The State University of New York, Buffalo, NY 14260-4200, United States

^b Fluid Metrology Group, National Institute of Standards and Technology, Gaithersburg, MD 20899-8360, United States

ARTICLE INFO

Article history:

Available online 15 February 2012

ABSTRACT

For helium-4, we present *ab initio*, semiclassical calculations of virial coefficients B_n for $n = 2, 3, 4$, and 5 from 50 to 1000 K. Using our values of B_4 and B_5 and the more accurate literature values of B_2 and B_3 , we argue that the *ab initio* virial equation of state is more accurate than recent, high-quality, densimeter measurements spanning the range $\{223 \text{ K} < T < 500 \text{ K}, p < 38 \text{ MPa}\}$. Thus, the present values of B_4 and B_5 extend the useful temperature and density range of *ab initio* helium standards.

© 2012 Elsevier B.V. All rights reserved.

1. Introduction

The virial equation of state, presented in Eq. (1), has long played an important role in metrology and molecular physics because of its connection to statistical mechanics. The virial coefficients B_n can be formulated rigorously in terms of molecular interaction energies, each encapsulating unique contributions to the pressure from interactions within groups of n molecules. This simple relation for the pressure p , temperature T , and molar density ρ , where N_A is the Avogadro constant, k_B is the Boltzmann constant, and Z is the compressibility factor, remains of high interest despite the typical restriction to low order n and thus low densities and pressures.

$$Z = \frac{p}{N_A k_B T \rho} = 1 + \sum_{n=2}^{\infty} B_n(T) \rho^{n-1} \quad (1)$$

For some time, the thermophysical properties of helium at low densities have been calculated from the *ab initio* virial equation of state more accurately than they can be measured; therefore, the calculated values have been used as standards to calibrate measuring instruments [1,2]. Several areas of gas metrology will benefit from extending accurate *ab initio* calculations to higher densities. These include: (1) a calculable pressure standard obtained by combining the *ab initio* equation of state with measurements of the temperature and density [3,4]; (2) calibration of the equation-of-state apparatus [5]; and (3) re-determination of the Boltzmann constant from measurements of the dielectric constant of helium at the temperature of the triple point of water [6].

To analyze experimental data, modifications to the virial equation of state are often employed. For example, to analyze data sets for helium, Moldover and McLinden [5] used the virial model for Z presented in Eq. (2):

$$Z = Z_{\text{ab initio}} + B_4 \rho^3 + \delta(T) + \frac{\varepsilon(T)}{\rho} \quad (2)$$

where

$$Z_{\text{ab initio}} = 1 + B_2 \rho + B_3 \rho^2$$

In Eq. (2), the small parameter ε accounts for zero offsets in the measurements of the pressure and the density. The small parameter δ accounts for the fact that experimental values of Z do not approach precisely 1 as pressure decreases. Values of $\delta \neq 0$ are generated by small errors in scale factors for measuring p , T , and ρ , as well as non-negligible impurity concentrations. Moldover and McLinden [5] used analytic representations of *ab initio* values of B_2 and B_3 in Eq. (2) and fitted values of δ , ε , and B_4 on each isotherm. In effect, fitting δ and ε calibrated the apparatus and protected the fitted values of B_4 from the imperfections associated with these terms. Their calibration reduced the uncertainty of the determination of B_4 by roughly a factor of 5 compared with a conventional calibration [7] that did not use *ab initio* values of B_2 and B_3 . Moldover and McLinden found that when an adjustable B_5 was included in fits to the measurements, it was not statistically different from zero; thus, any effect of B_5 and higher virials was implicitly included in their values of B_4 .

Here, we demonstrate that the Moldover–McLinden analysis of the experimental data can be significantly affected by the inclusion of an *ab initio* estimate of B_5 . The virial model that is fitted to provide B_4 this way includes an analytic representation of the fifth-order semiclassical values B_5^{SCL} reported in this work, as shown in Eq. (3).

$$Z = Z_{\text{ab initio}} + B_4 \rho^3 + \delta(T) + \frac{\varepsilon(T)}{\rho} \quad (3)$$

where

$$Z_{\text{ab initio}} = 1 + B_2 \rho + B_3 \rho^2 + B_5^{\text{SCL}} \rho^4$$

* Corresponding author. Fax: +1 716 645 3822.

E-mail address: kofke@buffalo.edu (D.A. Kofke).

Ab initio values of B_2 and B_3 are from [8] and [9], respectively. All *ab initio* values, including B_5^{SCL} , employ the pair potential of Pryzbytek et al. [10] and the nonadditive trimer potential of Cencek et al. [11]. Higher-order multi-body interactions are neglected. Garberoglio [12] showed that his *ab initio* calculation of B_4 using the centroid approximation and the same potentials is nearly consistent with the measurements of B_4 we determined in this manner and present here.

The fifth-order semiclassical values B_5^{SCL} reported here are computed by Mayer-sampling Monte Carlo (MSMC). MSMC has been applied previously to compute classical virial coefficients B_n^{CL} for a variety of potentials, including the Gaussian-charge polarizable model (GCPM) for water up to $n = 5$ [13], the Lennard–Jones potential up to $n = 8$ [14], and the flexible TraPPE-UA alkane models up to $n = 5$ [15,16]. The Lennard–Jones and TraPPE-UA potentials are pairwise additive, such that only the additive component B_n^{A} of the virial coefficient is relevant. For GCPM water or the nonadditive trimer interaction of Cencek et al. [11], one must also consider the nonadditive component B_n^{NA} .

Replacing the pair potential u_{12} with its quadratic Feynman–Hibbs (QFH) modification u_{12}^{QFH} [17–19], shown in Eq. (4), one can use the same MSMC framework to compute a semiclassical estimate of the additive component of the virial coefficient $B_n^{\text{A,SCL}}$ [20]. Here, h is Planck’s constant, \hbar is $h/(2\pi)$, and m is the mass of one of two identical atoms. In this work, we do not apply the QFH modification to the nonadditive trimer potential because of its complexity and its relatively minor contribution to the classical virial coefficients computed here.

$$u_{12}^{\text{QFH}}(r_{12}) = u_{12} + \frac{\hbar^2 \beta}{24(m/2)} \left[\frac{\partial^2 u_{12}}{\partial r_{12}^2} + \frac{2}{r_{12}} \frac{\partial u_{12}}{\partial r_{12}} \right] \quad (4)$$

As noted by Guillot and Guissani [19], Feynman–Hibbs effective potentials are more accurate and have better convergence properties than the Wigner–Kirkwood asymptotic expansion. In the Wigner–Kirkwood expansion, the first quantum correction is applied to the Boltzmann factor for the system of n particles. As described by Mayer and Band [21], the Wigner–Kirkwood expansion of the probability of a particular configuration can be viewed as approximating the use of a quantum correction to the potential energy $U_q - U$ within the exponential defining the probability: $e^{-\beta U_q} = e^{-\beta U} e^{-\beta(U_q - U)} \cong e^{-\beta U} (1 - \beta(U_q - U))$. Thus, employing a quantum correction directly to the potential should be more accurate.

We also consider the approach for the first quantum correction employed by Kim and Henderson [22,23], shown in Eq. (5), which we refer to as the KH approach. Here, g'_n is the n th density expansion coefficient of the classical radial distribution function g as defined by $g = e^{-\beta u_{12}} \sum_n g'_n \rho^n$ rather than $g = \sum_n g_n \rho^n$.

$$B_n^{\text{SCL}} = B_n^{\text{CL}} + (n-1) \frac{\hbar^2 \beta^2}{24\pi m} \times \int_0^\infty e^{-\beta u_{12}} g'_{n-2} \left[\frac{\partial^2 u_{12}}{\partial r_{12}^2} + \frac{2}{r_{12}} \frac{\partial u_{12}}{\partial r_{12}} \right] r_{12}^2 dr_{12} \quad (5)$$

This correction can be viewed as an approximation to the Wigner–Kirkwood expansion, in that the Boltzmann factor for only the 1–2 pair is corrected. The interactions between all other pairs are classical, and so we would expect the KH approach to perform worse at higher order n than the QFH approach. Kim and Henderson applied this approach to compute B_n^{SCL} for the additive Haberlandt potential of helium for $n = 2$ –4 [22] and $n = 5$ [23].

2. Calculation details

2.1. Notes on the potentials

Because the pair potential of Pryzbytek et al. [10] is unphysically negative at very short separations, we apply a supplemental hard core of $0.4 a_0$ to u_{12} and u_{12}^{QFH} (where a_0 is the Bohr radius). To compute u_{12}^{QFH} , we employ the mass of helium provided at the NIST website of 4.002602 amu. The nonadditive potential of Cencek et al. [11] is also unphysically negative at linear and near-linear configurations with very short separations, so we omit this energy if any of the pair separations is less than $2.5 a_0$.

For both the pair and nonadditive trimer potentials, we make no attempt to account for systematic errors in the potentials relative to true helium interactions; the uncertainties we report account only for Monte Carlo stochastic error. Garberoglio et al. [9] and Garberoglio [12] propagate uncertainties in the potential to the virial coefficients by examining respective positive and negative deviations of the potential, with magnitudes chosen to reflect the estimated accuracy of the potential. This carries an implicit assumption that inaccuracies in the potential at different separations are fully correlated. Apart from this, for $n = 2$, the approach has clear validity as a means to establish bounds on the accuracy of the virial coefficient: a more positive deviation in the potential will necessarily result in a more positive B_2 , and a more negative deviation will result in a more negative B_2 . At higher n , however, its validity is less clear because the virial coefficients are formed from sums of products of interaction terms of varying sign. Thus one could, for example, shift the potential up and find that the virial coefficient decreases. Moreover, errors in the potential may introduce errors in the coefficients that offset each other when summed to compute the pressure. Alternatively, one could examine the variance of B_n (or the pressure itself) upon application of repeated random perturbations of the potential. The result would be a type of confidence limit describing the effect of inaccuracies in the potential on the virial coefficients. In contrast to a simple shift of the potential, this treatment instead assumes that inaccuracies at different separations are completely uncorrelated, and in this respect the approach has drawbacks as well; we do not pursue it here either.

2.2. Calculations of classical and semiclassical approximations to B_n

For a spherically symmetric pair potential such as the helium potential of Pryzbytek et al., B_2 and B_3^{A} are readily computable by quadrature and fast Fourier transforms (FFT), respectively. Portions of higher-order additive components are also computable by FFT. To compute other terms, we employ the MSMC formulation that utilizes two-stage overlap sampling, described in detail elsewhere [13–16]. Two Monte Carlo calculations are employed: one in which the sampling weight is computed using the target integrand (the integrand of B_n evaluated using the helium pair potential) and another in which the sampling weight is computed using the reference integrand (the integrand of B_n evaluated for hard spheres having diameter 3 \AA).

Substantial savings in CPU time can be achieved with careful selection of which portion is computed by FFT, as demonstrated for the Lennard–Jones potential [24]. As in that work, we restrict the possibilities for $B_n^{\text{A,FFT}}$ to zero, or one of the four approximations that result from either the hypernetted chain (HNC) or the Percus–Yevick (PY) integral-equation theories applied through either the compressibility (c) or virial (v) equations: HNC(c), HNC(v), PY(c), and PY(v). We find that the PY(c) route affords the most efficient decomposition for the temperature range of 50–500 K, and compute

$B_n^A - B_n^{A,PY(C)}$ with 30 independent MSMC calculations of 10^8 steps each at both fourth and fifth orders.

The semiclassical approximations to B_n reported here employ only a classical nonadditive contribution: $B_n^{NA,CL}$. $B_n^{NA,CL}$ is computed using the MSMC method described by Benjamin et al. [13], but with simplifications accounting for the lack of uniquely four- and five-body interactions. We compute $B_3^{NA,CL}$ with 100 independent MSMC calculations of 10^6 steps, $B_4^{NA,CL}$ with 50 independent MSMC calculations of 10^6 steps, and $B_5^{NA,CL}$ with 30 independent MSMC calculations of 10^7 steps.

3. Results and discussion

3.1. Comparison with previous calculations of virial coefficients

Classical and semiclassical approximations to B_2 and B_3 are provided in Tables 1 and 2, respectively, and both B_4 and B_5 are given in Table 3. In Tables 2 and 3 the uncertainties of B_n^{CL} , $B_n^{SCL(QFH)}$, and $B_n^{SCL(KH)}$ account for the Monte Carlo stochastic error only, and for reasons discussed above in the section *Notes on the Potentials*, we do not attempt to account for the uncertainties from the helium pair and trimer potentials. In contrast, approximate uncertainties propagated from the potentials were reported in references [10] and [8] at the $k=2$ level for the values of B_3 in Table 2 and values of $B_4^{Centroid}$ in Table 3. We note that these uncertainty estimates are

roughly five times larger than the stochastic Monte Carlo uncertainties in this work.

The values of the classical and semiclassical approximations to B_2 , B_3 , B_4 , and B_5 are plotted for each order in Figure 1. One can see there that, at the considered temperatures, the QFH semiclassical approximation is in excellent agreement with the values for B_2 [25] and B_3 [9]. We should note that a different pair potential was used by Hurly and Mehl [25] in their computations of B_2 than is used in this work. Agreement is even better with the unpublished B_2 values [8] employing the pair potential of Przybytek et al. [10], presented at selected temperatures in Table 4. At the lowest temperature considered, 50 K, where the QFH semiclassical approximation is the least accurate, it yields an error of only -3.0% for B_2 and -0.8% for B_3 , whereas the classical estimate yields an error of -34.7% for B_2 and -19.0% for B_3 . For B_4 , the classical approximation has errors relative to the QFH semiclassical approximation of -29.3% at 50 K, -3.3% at 500 K, and -1.8% at 1000 K. For B_5 , these errors increase to -31.7% at 50 K, -5.2% at 500 K, and -4.0% at 1000 K.

Where considered here, the KH semiclassical approximation is slightly superior to the QFH semiclassical approximation for B_2 and B_3 , with the exception of B_2 at 50 K. The similarity of the results for both approximations reflects the relative smallness of the quantum effect. At temperatures lower than those considered here, there can be significant differences between the two. For B_4 , the semiclassical estimate $B_4^{SCL(QFH)}$ is in good agreement with

Table 1

The ^4He second virial coefficient B_2 .

T (K)	B_2^{CL} (cm^3/mol)	$B_2^{SCL(QFH)}$ (cm^3/mol)	$B_2^{SCL(KH)}$ (cm^3/mol)	B_2^a (cm^3/mol)
50	5.7231	8.4969	9.0752	8.7580
63.15	7.9222	9.9697	10.2887	
75	9.1180	10.7562	10.9627	
83.15	9.6933	11.1268	11.2860	
98.15	10.4287	11.5857	11.6907	
103.15	10.6086	11.6937	11.7864	
113.15	10.8992	11.8623	11.9358	
123.15	11.1185	11.9820	12.0415	
143.15	11.4105	12.1219	12.1628	
148.15	11.4612	12.1419	12.1795	
158.15	11.5428	12.1687	12.2006	
173.15	11.6258	12.1828	12.2083	
183.15	11.6609	12.1792	12.2014	
198.15	11.6908	12.1592	12.1775	
223.15	11.6968	12.0990	12.1126	
248.15	11.6666	12.0175	12.0280	
253.15	11.6575	11.9996	12.0095	
273.15	11.6137	11.9239	11.9322	
273.16	11.6137	11.9239	11.9321	11.9301
293.16	11.5607	11.8440	11.8509	
298.15	11.5464	11.8236	11.8303	11.8289
323.15	11.4699	11.7200	11.7254	
323.16	11.4699	11.7199	11.7254	
348.15	11.3879	11.6152	11.6197	
350	11.3817	11.6074	11.6119	11.6113
373.15	11.3027	11.5106	11.5144	
375	11.2963	11.5029	11.5067	11.5063
398.15	11.2159	11.4071	11.4104	
400	11.2094	11.3995	11.4028	11.4026
423.15	11.1285	11.3054	11.3082	
425	11.1221	11.2979	11.3007	
450	11.0350	11.1984	11.2008	11.2008
475	10.9487	11.1011	11.1032	
500	10.8635	11.0062	11.0081	11.0082
600	10.5381	10.6510	10.6521	10.6523
700	10.2397	10.3322	10.3331	10.3332
800	9.9677	10.0455	10.0461	10.0462
900	9.7194	9.7862	9.7867	9.7867
1000	9.4919	9.5502	9.5506	9.5505

^a Ref. [25].

Table 2

The ^4He third virial coefficient B_3 . Values in parentheses are standard ($k=1$) uncertainties on the rightmost digit(s).

T (K)	B_3^{CL} (cm^6/mol^2)	$B_3^{SCL(QFH)}$ (cm^6/mol^2)	$B_3^{SCL(KH)}$ (cm^6/mol^2)	B_3^a (cm^6/mol^2)
50	166.714(16)	204.174(16)	206.446(16)	205.82(11)
63.15	160.230(12)	189.914(12)	191.525(12)	191.03(10)
75	155.566(11)	180.155(11)	181.333(11)	180.98(8)
83.15	152.643(10)	174.484(10)	175.444(10)	
98.15	147.600(9)	165.514(9)	166.191(9)	
103.15	146.011(8)	162.866(8)	163.473(8)	
113.15	142.940(7)	157.958(7)	158.451(7)	
123.15	139.996(7)	153.484(7)	153.890(7)	
143.15	134.513(6)	145.609(6)	145.894(6)	
148.15	133.228(5)	143.835(5)	144.097(5)	
158.15	130.715(5)	140.441(5)	140.666(5)	
173.15	127.155(5)	135.768(5)	135.947(5)	
183.15	124.898(5)	132.880(5)	133.036(5)	
198.15	121.695(5)	128.863(5)	128.991(5)	
223.15	116.788(4)	122.871(4)	122.966(4)	
248.15	112.332(4)	117.575(4)	117.647(4)	
253.15	111.494(5)	116.591(5)	116.660(5)	
273.15	108.285(4)	112.862(4)	112.919(4)	
273.16	108.275(4)	112.853(4)	112.909(4)	112.93(3)
293.16	105.290(4)	109.429(4)	109.476(4)	
298.15	104.575(4)	108.615(4)	108.659(4)	
323.15	101.171(4)	104.769(4)	104.805(4)	
323.16	101.166(3)	104.763(3)	104.799(3)	
348.15	98.016(4)	101.246(4)	101.276(4)	
350	97.801(3)	101.006(3)	101.035(3)	101.04(3)
373.15	95.105(4)	98.024(4)	98.049(4)	
375	94.906(4)	97.805(4)	97.829(4)	97.86(3)
398.15	92.392(3)	95.047(3)	95.068(3)	
400	92.211(3)	94.848(3)	94.868(3)	94.88(3)
423.15	89.871(4)	92.298(4)	92.316(4)	
425	89.691(4)	92.103(4)	92.120(4)	
450	87.343(4)	89.559(4)	89.574(4)	89.59(3)
475	85.133(3)	87.177(3)	87.190(3)	
500	83.061(3)	84.955(3)	84.966(3)	84.97(3)
600	75.848(3)	77.287(3)	77.293(3)	77.30(3)
700	69.963(3)	71.101(3)	71.105(3)	71.13(2)
800	65.064(3)	65.990(3)	65.993(3)	66.01(2)
900	60.895(3)	61.667(3)	61.669(3)	61.68(2)
1000	57.297(3)	57.951(3)	57.953(3)	57.97(2)

^a Ref. [10]. These values include propagated uncertainties in the potential.

Table 3

The ^4He fourth and fifth virial coefficients B_4 and B_5 . Values in parentheses are standard ($k = 1$) uncertainties on the rightmost digit(s).

T (K)	B_4^{CL} (cm^9/mol^3)	$B_4^{\text{SCL(QFH)}}$ (cm^9/mol^3)	$B_4^{\text{Centroida}}$ (cm^9/mol^3)	B_5^{CL} ($\text{cm}^{12}/\text{mol}^4$)	$B_5^{\text{SCL(QFH)}}$ ($\text{cm}^{12}/\text{mol}^4$)
50	1574.4(2)	2227.9(2)		$1.737(3) \times 10^4$	$2.5420(17) \times 10^4$
63.15	1542.01(19)	2010.4(2)		$1.4907(16) \times 10^4$	20028(10)
75	1477.24(13)	1839.03(14)		$1.2947(11) \times 10^4$	16593(7)
83.15	1427.05(13)	1735.82(14)		11796(6)	14773(6)
98.15	1333.85(13)	1571.67(14)		10045(4)	12190(4)
103.15	1303.77(13)	1523.44(14)		9551(3)	11492(3)
113.15	1246.25(11)	1435.68(11)		8674(2)	10278(4)
123.15	1191.85(11)	1356.91(12)		7918(3)	9265(3)
143.15	1094.45(11)	1223.01(11)		6690.5(17)	7678(2)
148.15	1072.27(11)	1193.83(11)		6426(2)	7348.4(19)
158.15	1030.04(12)	1139.01(12)		5951.6(18)	6757(2)
173.15	972.20(10)	1065.57(10)		5340.8(15)	6004.4(17)
183.15	936.53(9)	1021.53(9)		4984.4(13)	5572.0(14)
198.15	887.71(11)	961.99(11)		4511.9(16)	5012.5(13)
223.15	816.34(9)	876.75(9)		3870.5(13)	4256.5(15)
248.15	755.04(9)	805.31(9)		3357.8(11)	3663.4(12)
253.15	743.68(9)	792.24(9)		3269.3(11)	3560.7(12)
273.15	701.51(10)	743.97(10)		2940.8(11)	3187.9(12)
273.16	701.44(8)	743.88(8)	744.7(5)	2940.0(14)	3186.4(11)
293.16	663.56(8)	701.02(8)		2659.2(11)	2870.0(11)
298.15	654.87(9)	691.24(9)		2595.7(9)	2798.7(10)
323.15	613.65(8)	645.13(8)		2305.1(10)	2476.1(9)
323.16	613.66(8)	645.16(8)		2305.7(10)	2474.4(10)
348.15	576.93(7)	604.45(7)		2063.2(10)	2206.3(9)
350	574.52(7)	601.81(7)	601.8(5)	2046.1(12)	2186.5(13)
373.15	544.31(7)	568.59(8)		1852.3(8)	1974.0(9)
375	541.96(6)	566.01(6)	566.1(5)	1837.5(9)	1957.9(9)
398.15	514.76(8)	536.34(8)		1672.1(9)	1777.3(9)
400	512.81(7)	534.21(7)	534.1(5)	1658.7(10)	1763.1(9)
423.15	488.05(6)	507.36(6)		1516.0(8)	1607.0(8)
425	486.15(6)	505.31(6)		1504.5(8)	1594.7(9)
450	462.32(10)	479.56(10)	479.2(5)	1367.7(13)	1446.3(13)
475	440.02(6)	455.60(6)	455.5(5)	1247.7(8)	1315.5(8)
500	420.04(6)	434.19(6)	433.8(4)	1140.1(7)	1202.1(7)
600	353.34(7)	363.41(7)	363.2(4)	815.6(7)	855.3(7)
700	303.35(5)	310.86(5)	310.8(4)	597.0(7)	623.9(7)
800	264.60(6)	270.41(6)	270.1(4)	443.6(5)	463.0(5)
900	233.38(5)	238.01(5)	237.8(4)	330.6(6)	344.9(7)
1000	208.04(5)	211.78(5)	211.6(4)	247.7(4)	258.0(4)

^a Ref. [12]. These values include propagated uncertainties in the nonadditive trimer potential.

the centroid approximation of Garberoglio [12], as can be seen in Table 3 and in Figure 1c. While quantitative comparison is limited by consideration of different temperatures, the values differ by less than 0.11% at 273.16 K and above. $B_4^{\text{SCL(QFH)}}$ is more positive than B_4^{Centroid} at temperatures above 400 K, and more negative at temperatures below 350 K. While the accuracy of B_4^{Centroid} is unknown, the accuracy of B_3^{Centroid} is worse below room temperature than the semiclassical approximation [12].

Components of the classical and semiclassical approximations to B_4 and B_5 are plotted in Figure 2. For the temperature range of interest, the PY(c) approximation is the largest component of the total value. The errors of this approximation for B_4 range from -2.5% at 50 K to 8.6% at 500 K and for B_5 range from -11.4% at 50 K to 56.0% at 500 K. The PY(c) approximation is known to worsen with increasing order n , but perhaps could still provide an order-of-magnitude estimate of B_6 . The PY(c) approximation, which is a subset of the additive component, becomes worse with increasing temperature because the additive component as a whole diminishes to a value closer to that of the nonadditive component, which has a weak temperature dependence in this range. The nonadditive component is most significant at high temperature where quantum effects are unimportant.

3.2. Comparison with measurements

Instead of focusing on a particular virial coefficient, we ask: are the helium data consistent with the *ab initio* equation of state including semiclassical B_4 and B_5 ? To answer this question, we fitted the two instrument parameters $\delta(T)$ and $\varepsilon(T)$ on each isotherm using Eq. (6), where $B_2(T)$ and $B_3(T)$ are analytic representations of the values from [8] and [9], respectively, and semiclassical $B_4(T)$ and $B_5(T)$ are analytic representations of the values computed in this work. (The deviations of the tabulated numerical values from the analytic representations were random and of the same order as the uncertainty in the values.)

$$Z = Z_{\text{ab initio}} + \delta(T) + \frac{\varepsilon(T)}{\rho} \quad (6)$$

where

$$Z_{\text{ab initio}} = 1 + B_2\rho + B_3\rho^2 + B_4^{\text{SCL(QFH)}}\rho^3 + B_5^{\text{SCL(QFH)}}\rho^4$$

We consider two sets of helium data: the isotherms of McLinden and L6sch–Will [7] and those of Moldover and McLinden [5]. We refer to these as the ‘ML isotherms’ and the ‘MM isotherms’, respectively. (Moldover and McLinden [5] referred to these as the ‘2005 isotherms’ and ‘2007 isotherms’, respectively.) Table 4 lists the fitted values of δ and ε , and the previously unpublished values of B_2 from [9]. For both the ML and MM isotherms, the deviations of the fitted values of Z from the experimental values are plotted at selected temperatures from 223 to 500 K in Figure 3. The standard deviation of the error in fitted Z is 1.06×10^{-5} , which is slightly larger than the value 0.98×10^{-5} reported by Moldover and McLinden [5]. This is not surprising because in [5] they fitted a third parameter, B_4 , to the data on each isotherm. We also considered the effect of the uncertainty of the isothermal compressibility $u(\kappa_T)$ of the ‘sinks’ used to measure the density of the helium. McLinden and L6sch–Will [7] conservatively estimate the relative uncertainty from this source as $u_r(\rho) = 1.3 \times 10^{-6} (p/\text{MPa})$. Upon changing the measured values of ρ by the factor $[1 - 0.4 \times 10^{-6} (p/\text{MPa})]$ which is 30% of $u_r(\rho)$, the standard deviation decreased to 0.99×10^{-5} , essentially the same value reported by Moldover and McLinden.

From Figure 3, we conclude that the *ab initio* virial equation of state is consistent with the densimeter measurements throughout the temperature range 223–500 K at pressures up to 38 MPa. Before calibration, the standard deviation of data in Figure 3 above 7 MPa was 3.7×10^{-5} , which is smaller than expected from the densimeter’s specifications. (Sections 3.4, 3.5, and 3.6 of [7] discuss the uncertainties of the densimeter measurements before calibration with helium. The uncertainties are a complicated function of the temperature, pressure, and density of the test fluid. For helium at 293 K and 20 MPa, $u_r(\rho) \approx 5 \times 10^{-5}$; the uncertainty is larger at higher and lower pressures and at higher and lower temperatures.) We conclude that the present virial model is indeed useful for reducing the uncertainty of the densimeter measurements. By fitting the parameters $\delta(T)$ and $\varepsilon(T)$, Moldover and McLinden calibrated out the imperfections of the apparatus at low pressures. By fitting κ_T , we demonstrate the possibility of calibrating out other imperfections at high pressures. (An apparent, linear pressure dependence of the density might result from some combination of an error in κ_T , a systematic error in the pressure calibration, or hysteresis in the pressure transducer.)

We now consider the possible effects of our neglect of B_6 for two thermodynamic states: (1) the highest density ($0.002762 \text{ mol cm}^{-3}$ at 7 MPa) on the 273.16 K isotherm that was used by Fellmuth et al. [6] during their recent determination of k_B , and (2), the lowest temperature and highest density in the densimeter measurements

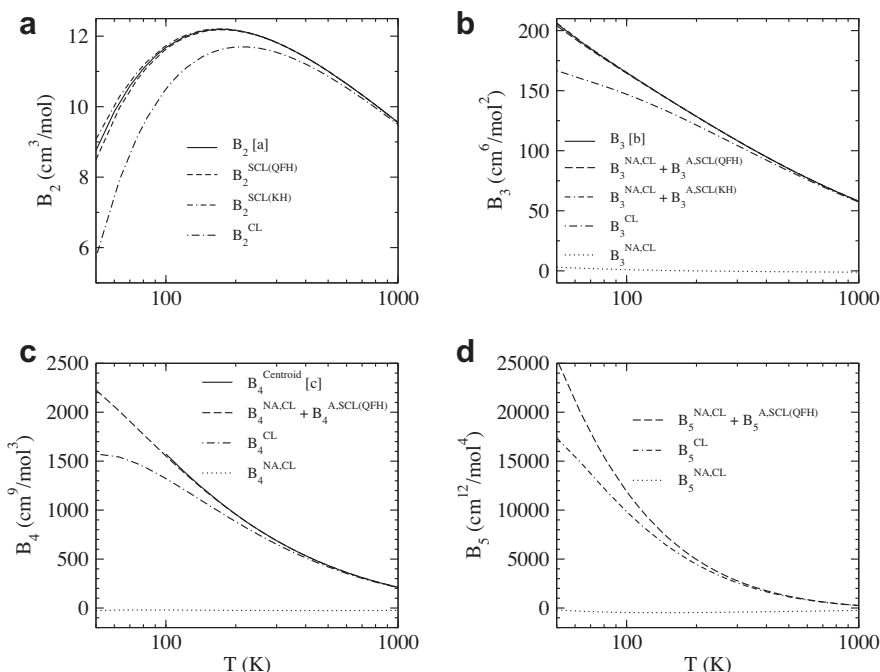


Figure 1. Comparison of semiclassical and classical approximations to the ^4He virial coefficients at (a) second, (b) third, (c) fourth, and (d) fifth order. At second and third order, available quantum values are shown to be in excellent agreement with the semiclassical approximations. At third and higher order, the nonadditive component is also plotted to show its relatively small contribution. Error bars denoting standard ($k = 1$) uncertainties are too small to be discernable. (a) Ref. [25], (b) Ref. [9] and (c) Ref. [12].

Table 4

Values of the fitting parameters $\varepsilon(T)$ and $\delta(T)$ in Eq. (6) and their standard ($k = 1$) uncertainties. Also presented are values of B_2 from [8] used in Eq. (6), with their expanded ($k = 2$) uncertainties indicated by the digits in parentheses.

T (K)	$10^4 \varepsilon$ (kg/m ³)	$10^6 \delta$	B_2 (cm ³ /mol)
<i>ML isotherms</i> ^a			
223.14	-2.01(36)	-73(3)	12.1056(12)
253.15	-0.78(35)	-43(4)	12.0044(11)
273.16	-4.51(80)	-42(6)	11.9279(10)
273.16	-4.20(36)	-22(4)	
273.16	1.42(38)	-27(5)	
273.16	-1.56(30)	-24(3)	
293.16	-6.22(48)	-12(6)	11.8474(9)
323.16	-9.37(19)	48(3)	11.7226(9)
<i>MM isotherms</i> ^b			
323.16	0.54(1.00)	10(7)	
323.16	-3.26(1.27)	14(9)	
350.01	-1.89(1.39)	22(11)	11.6095(8)
375.01	1.91(0.83)	22(7)	11.5047(8)
400.01	2.84(1.17)	-2(10)	11.4011(7)
425.01	7.75(0.68)	-33(4)	11.2992(7)
450.01	-2.67(0.61)	4(6)	11.1995(7)
475.00	-7.33(0.63)	22(6)	11.1021(6)
500.01	-11.23(1.27)	30(13)	11.0071(6)

^a Ref. [7].

^b Ref. [5].

of McLinden and Lösch-Will [7] shown in Figure 3. At 273.16 K and $0.0027629 \text{ mol cm}^{-3}$, the terms $B_2\rho$, $B_3\rho^2$, $B_4^{\text{SCL}}\rho^3$, and $B_5^{\text{SCL}}\rho^4$ have the values 0.032955, 0.861×10^{-3} , 1.6×10^{-5} , 1.86×10^{-7} , respectively. Thus, the virial series converges rapidly and a reasonable guess is $B_6\rho^5 \approx 2 \times 10^{-9}$ [26]. Also, at 273.16 K and $0.0027629 \text{ mol cm}^{-3}$, we have the $k = 1$ uncertainties $u(B_2)\rho = 1.7 \times 10^{-6}$ from [9], $u(B_3)\rho^2 = 2.4 \times 10^{-7}$ from [10], and $u(B_4)\rho^3 = 1.1 \times 10^{-8}$ from [12] (all of which are dominated by contributions that attempt to estimate effects of possible inaccuracy in the *ab initio* potentials). Thus all of the terms $B_6\rho^5$,

$u(B_2)\rho \cdot \dots \cdot u(B_5)\rho^4$ at 273.16 K and 7 MPa are much smaller than the relative uncertainty $u_r(k_B) = 7.9 \times 10^{-6}$ claimed for the Boltzmann constant measurement in [6].

At 223.15 K and $0.01664 \text{ mol cm}^{-3}$, the terms $B_2\rho$, $B_3\rho^2$, $B_4^{\text{SCL}}\rho^3$, and $B_5^{\text{SCL}}\rho^4$ have the values 0.2015, 0.03403, 4.04×10^{-3} , 3.27×10^{-4} , respectively; therefore, we estimate $B_6\rho^5 \approx 2 \times 10^{-5}$ [26], which is larger than 1.06×10^{-5} , the standard deviation of the data in Figure 3. However, numerical experiments show that adding the term $2 \times 10^{-5} (\rho/0.01664 \text{ mol cm}^{-3})^5$ to the 223.15 K isotherm and refitting δ and ε would not make the 223.15 K isotherm stand out in Figure 3. Also at 223.15 K and $0.01664 \text{ mol cm}^{-3}$, we have the $k = 1$ uncertainties $u(B_2)\rho = 0.98 \times 10^{-5}$ from [9], $u(B_3)\rho^2 = 0.97 \times 10^{-5}$ from [10], $u(B_4)\rho^3 = 0.04 \times 10^{-5}$ from Table 3 (or 0.12×10^{-5} if using the uncertainty in [12], which attempts a contribution for inaccuracy in the potential), and $u(B_5)\rho^4 = 0.01 \times 10^{-5}$ also from Table 3. The sum in quadrature of the terms $u(B_n)\rho^{n-1}$ is $\sim 1.4 \times 10^{-5}$, which is smaller than the estimated error incurred from neglect of $B_6\rho^5$ but larger than the standard deviation in the data. To summarize, the error in the *ab initio* virial equation of state of helium at 223.15 K and $0.01664 \text{ mol cm}^{-3}$ is approximately 2.0 times larger than the resolution of a contemporary, accurate, densimeter; however, the densimeter could not detect an error of this size in the equation of state of helium because the values of the fitted apparatus parameters $\delta(T)$ and $\varepsilon(T)$ (and possibly κ_T) would change to accommodate it. Thus, we assert that the *ab initio* equation of state of helium is more accurate than this densimeter in the range of the MM and ML data.

In [12], Garberoglio used the same densimeter data to ask a different question: what values of B_4 result from the data when the instrumental parameters $\delta(T)$ and $\varepsilon(T)$ are allowed to vary while B_2 is fixed at the *ab initio* values in [9], B_3 is fixed at the *ab initio* values in [8], and B_5 is fixed at the semi-classical values reported in this work? This question is answered in Table 5. For comparison, Table 5 also displays the values of $B_4^{\text{SCL(QFH)}}$ computed here, and the values of B_4 fitted to experiment by Moldover and McLinden using

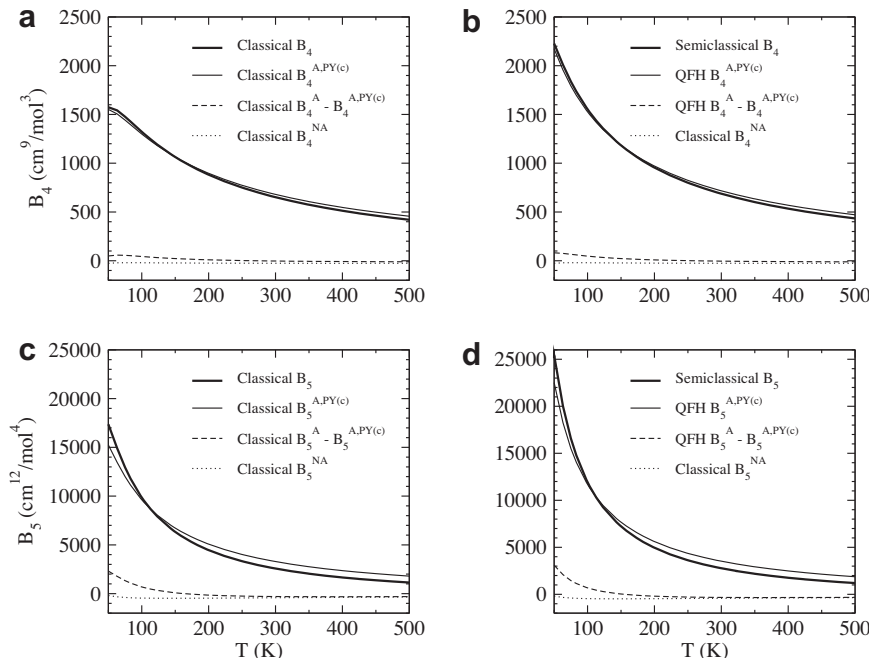


Figure 2. Components of (a) B_4^{CL} , (b) $B_4^{\text{SCL(QFH)}}$, (c) B_5^{CL} , and (d) $B_5^{\text{SCL(QFH)}}$ for ^4He . The additive Percus–Yeick compressibility-route approximation, computable by FFT, is the largest component in all cases. Error bars denoting standard ($k = 1$) uncertainties are too small to be discernable.

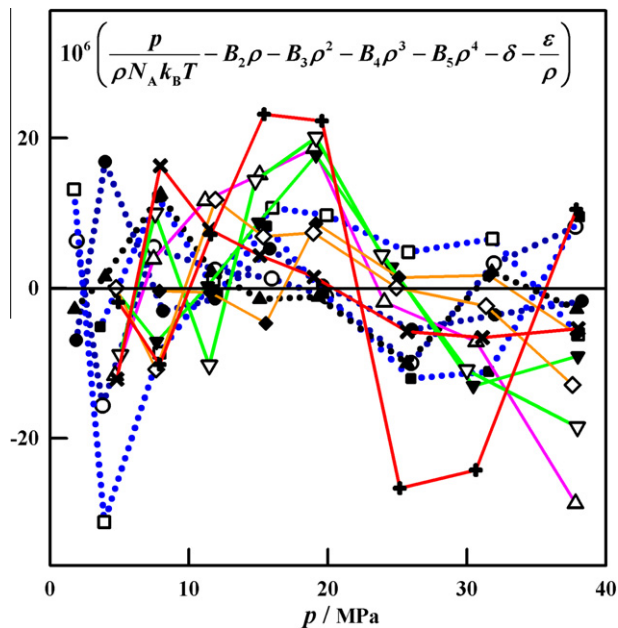


Figure 3. Relative deviations of measured data from the virial model (Eq. (6)) after fitting values of the apparatus parameters δ and ϵ on each isotherm. The data from [5] are linked by solid lines; the data from [7] are linked by dotted lines. The standard deviation of the data is 10.6×10^{-6} . The symbols identifying the isotherms are: ● 223 K; ○ 253 K; ■ 273 K; □ 293 K; ▲ 323 K; △ 350 K; ▼ 375 K; ▽ 400 K; ◆ 425 K; ◇ 450 K; × 475 K; + 500 K.

the assumption that $B_5 \cong 0$. The results trend differently for the ML and MM data sets. When $B_5^{\text{SCL(QFH)}}$ is used, the fitted values of B_4 for the ML isotherms agree within combined uncertainties with $B_4^{\text{SCL(QFH)}}$ (as well as B_4^{centroid} (not shown)); including $B_5^{\text{SCL(QFH)}}$ brings the fitted values of B_4 into much better agreement with the *ab initio* estimates. However, the values of B_4 obtained by fitting the MM isotherms differ from the *ab initio* values such that on average

Table 5

The ^4He fourth virial coefficient B_4 fitted using virial models, compared to the semiclassical $B_4^{\text{SCL(QFH)}}$ values at some of the temperatures computed in this work. Values in parentheses are standard ($k = 1$) uncertainties on the rightmost digit(s).

T (K)	$B_4^{\text{SCL(QFH)}}$ (cm^9/mol^3)	B_4 fitted with $B_5^{\text{SCL(QFH)}}$ included (cm^9/mol^3)	B_4 fitted in [5] with $B_5 \equiv 0$ (cm^9/mol^3)
<i>ML Isotherms</i> [7]			
223.14	876.75(9)	875.1(2.0)	960(12)
253.15	792.24(9)	795(3.1)	864(14)
273.16	743.88(8)	743.2(5.1)	801(14)
273.16	743.88(8)	735.7(2.9)	791(15)
273.16	743.88(8)	746.3(4.7)	803(15)
273.16	743.88(8)	739.9(3.3)	799(16)
293.16	701.02(8)	702.4(8.0)	750(17)
323.16	645.16(8)	641.6(4.2)	674(19)
<i>MM isotherms</i> [5]			
323.16	645.16(8)	623.7(3.0)	659(17)
323.16	645.16(8)	619.5(3.6)	661(17)
350	601.81(7)	563.1(4.6)	593(19)
375	566.01(6)	546.8(10.3)	573(22)
400	534.21(7)	496.3(15.2)	521(25)
425	505.31(6)	493.3(9.5)	512(24)
450	479.56(10)	447.9(12.9)	465(31)
475	455.60(6)	425.4(18.8)	442(36)
500	434.19(6)	412.7(55.6)	427(53)

$B_{4,\text{MM}} - B_4^{\text{SCL(QFH)}} = -25 \text{ cm}^9/\text{mol}^3$, and at most temperatures, including $B_5^{\text{SCL(QFH)}}$ worsens the agreement of the fitted values with the *ab initio* estimates. At this point we are not prepared to draw conclusions about the origin of this differing behavior, but it is worthwhile to consider possible causes. We note first that while this difference is comparable to the measurement uncertainty, it is biased and thus suggests an inaccuracy (i.e., systematic error). Such an error in the *ab initio* virial coefficients could result from the neglect of 4- or 5-body contributions to the potential, or it could be inherent in the 2- and 3-body potentials used to calculate the virial coefficients. In this respect we note that Garberoglio's

confidence limits, which attempt also to characterize the magnitude of the bias in B_4^{centroid} that could result from inaccuracies in the 3-body potential, are only about $1 \text{ cm}^9/\text{mol}^3$, and thus do not explain the deviation observed in Table 5. Alternatively it may have to do with neglect of B_6 , or it could reflect some subtle issue with the experimental data. Further study should be able to resolve the question.

4. Conclusions

The helium equation-of-state data from McLinden and Lösch-Will [7] and Moldover and McLinden [5] are consistent with the virial equation of state using *ab initio* values of B_2 , B_3 , $B_4^{\text{SCL(QFH)}}$, and $B_5^{\text{SCL(QFH)}}$, together with reasonable values of the temperature-dependent apparatus parameters δ and ϵ . We detected a possible correction to the isothermal compressibility of the sinkers corresponding to about one-third of its uncertainty estimated from the literature. If the uncertainties of the calculated virial coefficients are uncorrelated and if four and five-body interactions can be ignored, the ($k = 1$) relative uncertainty of the calculated density is approximately 2.5×10^{-5} in the worst case considered here. Under these conditions (223 K, 38 MPa), the theoretical uncertainty is smaller than the uncertainty of the best measurements known to the authors.

At the considered temperatures, the semiclassical values of the virial coefficients of helium as computed here constitute a significant improvement relative to the classical approximation. We plan to compute fourth and fifth virial coefficients fully accurate with respect to quantum effects such that lower temperatures can be considered. While the nonadditive trimer contributions are relatively small at all orders relative to the total virial coefficient, the significance of the four- and five-body interactions is unknown and merits further investigation.

Acknowledgements

The authors thank J. B. Mehl and G. Garberoglio for sharing their results for B_2 and B_4 , respectively, with us before publication. This

material is based upon work supported by the US National Science Foundation under Grant No. CHE-1027963. Calculations were performed using resources from the University at Buffalo Center for Computational Research.

References

- [1] R.A. Aziz, A.R. Janzen, M.R. Moldover, Phys. Rev. Lett. 74 (1995) 1586.
- [2] E.F. May, M.R. Moldover, R.F. Berg, J.J. Hurly, Metrologia 43 (2006) 247.
- [3] M.R. Moldover, J. Res. Natl. Inst. Stan. 103 (1998) 167.
- [4] J.W. Schmidt, R.M. Gavioso, E.F. May, M.R. Moldover, Phys. Rev. Lett. 98 (2007) 254504.
- [5] M.R. Moldover, M.O. McLinden, J. Chem. Thermodyn. 42 (2010) 1193.
- [6] B. Fellmuth, J. Fischer, C. Gaiser, O. Jusko, T. Priruenrom, W. Sabuga, et al., Metrologia 48 (2011) 382.
- [7] M.O. McLinden, C. Lösch-Will, J. Chem. Thermodyn. 39 (2007) 507.
- [8] W. Cencek, M. Przybytek, J. Komasa, J.B. Mehl, B. Jeziorski, K. Szalewicz, Private communication from James B. Mehl (2011).
- [9] G. Garberoglio, M.R. Moldover, A.H. Harvey, J. Res. Natl. Inst. Stan. 116 (2011) 729.
- [10] M. Przybytek, W. Cencek, J. Komasa, G. Lach, B. Jeziorski, K. Szalewicz, Phys. Rev. Lett. 104 (2010) 183003.
- [11] W. Cencek, K. Patkowski, K. Szalewicz, J. Chem. Phys. 131 (2009) 064105.
- [12] G. Garberoglio, Chem. Phys. Lett. 525–526 (2012) 19.
- [13] K.M. Benjamin, A.J. Schultz, D.A. Kofke, J. Phys. Chem. B 113 (2009) 7810.
- [14] A.J. Schultz, D.A. Kofke, Mol. Phys. 107 (2009) 2309.
- [15] A.J. Schultz, D.A. Kofke, J. Chem. Phys. 133 (2010) 104101.
- [16] K.R.S. Shaul, A.J. Schultz, D.A. Kofke, J. Chem. Phys. 135 (2011) 124101.
- [17] R.P. Feynman, A.R. Hibbs, Quantum Mechanics and Path Integrals, McGraw-Hill, New York, 1965.
- [18] R.P. Feynman, Statistical Mechanics; A Set of Lectures, W. A. Benjamin, Reading, MA, 1972.
- [19] B. Guillot, Y. Guissani, J. Chem. Phys. 108 (1998) 10162.
- [20] G.K. Schenter, J. Chem. Phys. 117 (2002) 6573.
- [21] J.E. Mayer, W. Band, J. Chem. Phys. 15 (1947) 141.
- [22] S. Kim, D. Henderson, Proc. Natl. Acad. Sci. USA 55 (1966) 705.
- [23] S. Kim, D. Henderson, Chem. Phys. Lett. 2 (1968) 619.
- [24] K.R.S. Shaul, A.J. Schultz, A. Perera, D.A. Kofke, Mol. Phys. 109 (2011) 2395.
- [25] J.J. Hurly, J.B. Mehl, J. Res. Natl. Inst. Stan. 112 (2007).
- [26] This estimate, rounded to one significant figure, agrees with estimates corresponding to the Percus–Yevick compressibility-route approximation to the classical sixth virial coefficient and the classical sixth virial coefficient employing the Haberlandt potential for helium (R. Haberlandt, Phys. Lett. 8 (1964) 172; R. Haberlandt, Phys. Lett. 14 (1965) 197). Given its imprecision and the associated temperature, quantum contributions are not significant to this estimate.